Sweet taste receptors in rat small intestine stimulate glucose absorption through apical GLUT2

Oliver J. Mace, Julie Affleck, Nick Patel and George L. Kellett

Department of Biology (Area 3), University of York, York YO10 5YW, UK

Natural sugars and artificial sweeteners are sensed by receptors in taste buds. T2R bitter and T1R sweet taste receptors are coupled through G-proteins, α-gustducin and transducin, to activate phospholipase C β2 and increase intracellular calcium concentration. Intestinal brush cells or solitary chemosensory cells (SCCs) have a structure similar to lingual taste cells and strongly express α-gustducin. It has therefore been suggested over the last decade that brush cells may participate in sugar sensing by a mechanism analogous to that in taste buds. We provide here functional evidence for an intestinal sensing system based on lingual taste receptors. Western blotting and immunocytochemistry revealed that all T1R members are expressed in rat jejunum at strategic locations including Paneth cells, SCCs or the apical membrane of enterocytes; T1Rs are colocalized with each other and with α-gustducin, transducin or phospholipase C β2 to different extents. Intestinal glucose absorption consists of two components: one is classical active Na^+–glucose cotransport, the other is the diffusive apical GLUT2 pathway. Artificial sweeteners increase glucose absorption in the order acesulfame potassium $\sim$ sucralose $>$ saccharin, in parallel with their ability to increase intracellular calcium concentration. Stimulation occurs within minutes by an increase in apical GLUT2, which correlates with reciprocal regulation of T1R2, T1R3 and α-gustducin *versus* T1R1, transducin and phospholipase C β2. Our observation that artificial sweeteners are nutritionally active, because they can signal to a functional taste reception system to increase sugar absorption during a meal, has wide implications for nutrient sensing and nutrition in the treatment of obesity and diabetes.

(Received 22 February 2007; accepted after revision 10 May 2007; first published online 10 May 2007)
Corresponding author: G. L. Kellett: Department of Biology (Area 3), University of York, York YO10 5YW, UK.
Email: glk1@york.ac.uk

Intestinal glucose absorption occurs either via the classical pathway of active transport mediated by the Na^+–glucose cotransporter SGLT1, or the apical GLUT2 pathway, which at high concentrations of sugar can be 3- to 5-times greater than by SGLT1. The apical GLUT2 pathway is mediated by glucose-induced insertion of GLUT2 into the apical membrane, thereby providing a cooperative mechanism by which glucose absorptive capacity is rapidly and precisely matched to dietary intake immediately after a meal (Kellett & Helliwell, 2000; Helliwell *et al.* 2000*a*,*b*; Kellett, 2001; Kellett & Brot-Laroche, 2005). Apical GLUT2 also provides a pathway of fructose entry in addition to that by GLUT5.

The apical GLUT2 pathway is conserved in species from insects (Caccia *et al.* 2005, 2007) to humans (Kwon *et al.* 2006). It is abolished in GLUT2-null mice (Gouyon *et al.* 2003) and is regulated by experimental diabetes (Corpe *et al.* 1996), entero-endocrine sensing through glucagon like peptide (GLP-2) (Au *et al.* 2002), energy sensing by activated protein kinase (AMPK) (Walker *et al.* 2004), refeeding after starvation (Habold *et al.* 2005), long-term dietary carbohydrate intake (Gouyon *et al.* 2003) and development (Baba *et al.* 2005). Two signals mediate the regulation of the apical GLUT2 pathway by glucose. One is dietary Ca^{2+}: thus depolarization of the apical membrane by transport of glucose through SGLT1 stimulates Ca^{2+} entry via the L-type channel $Ca_v1.3$ to cause contraction of the terminal web, which is essential for insertion (Morgan *et al.* 2003, 2007; Mace *et al.* 2007). However, little insertion occurs at low glucose concentrations (20 mM), even when the entry of Ca^{2+} is strongly stimulated; a second unknown signal must therefore occur at concentrations of glucose above the 30 mM required to saturate SGLT1, where the apical GLUT2 component predominates (Kellett & Helliwell, 2000).

Rodent small intestine contains brush cells (Hofer *et al.* 1996), which are one form of solitary chemosensory cells (SCCs) (Sbarbati & Osculati, 2005). Brush cells have a structure similar to lingual taste cells and strongly express the G-protein α-gustducin (Hofer *et al.* 1996). It has therefore been suggested over the last decade that brush cells may participate in sugar sensing by a mechanism analogous to that in taste buds

 DOI: 10.1113/jphysiol.2007.130906

(Raybould, 1998; Hofer *et al.* 1999). During this time, the importance of G-protein-coupled receptors (GPCRs) in nutrient sensing has become increasingly recognized; for example, in the detection of lipid by GPR40 and of calcium and L-amino acids by the calcium-sensing receptor (Dockray, 2003; Itoh *et al.* 2003; Conigrave & Brown, 2006). Fresh impetus has been given to the analogy of intestinal sensing and taste reception by the discovery of the T2R bitter and the T1R sweet taste receptor families (Adler *et al.* 2000; Montmayeur *et al.* 2001; Nelson *et al.* 2001; Li *et al.* 2002). Both T2R and T1R receptors are GPCRs coupled to α-gustducin and/or transducin, through which they can activate a phospholipase C (PLC) $\beta 2$-dependent pathway to increase intracellular Ca^{2+} concentration; T1R receptors may also activate a cAMP-dependent pathway (Margolskee, 2002). T1R family members act in combination (Li *et al.* 2002): the T1R1 + T1R3 heterodimer senses amino acid and umami taste, whereas T1R2 + T1R3 senses sweet taste. Simple sugars, such as glucose, fructose and sucrose, invoke maximal increase in intracellular Ca^{2+} levels at concentrations up to several hundred millimolar, whereas artificial sweeteners, including acesulfame potassium, sucralose and saccharin, act at concentrations of a few millimolar (Li *et al.* 2002).

Mouse intestine expresses T2R receptor transcripts and stimulation of Ca^{2+} entry into entero-endocrine STC-1 cells by bitter taste stimuli may occur through $Ca_v1.3$ channels (Wu *et al.* 2002; Chen *et al.* 2006). Moreover, sheep intestine expresses a sugar sensor involved in the synthesis of SGLT1, but which is distinct from SGLT1 (Dyer *et al.* 2003). Accordingly, we noted that sweet taste receptors in tongue respond to sugars in the same high concentration range, 30–100 mM, as the unknown signal we were searching for in the regulation of apical GLUT2 (Kellett & Helliwell, 2000; Li *et al.* 2002; Mace *et al.* 2007).

Methods

Intestinal perfusion

Male Wistar rats (240–270 g) were fed standard Bantin and Kingman (Hull, UK) rat and mouse diet *ad libitum* with free access to water. For jejunal perfusion *in vivo* (Kellett & Helliwell, 2000; Morgan *et al.* 2007), rats were anaesthetized by an intraperitoneal injection of a mixture of 1.0 ml (kg body weight)$^{-1}$ Hypnorm (Janssen, UK) and 0.4 ml (kg body weight)$^{-1}$ Hypnovel (Roche, UK). A mid to distal loop of jejunum was cannulated at 10 and 35 cm from the Ligament of Treitz and perfused *in vivo* in single-pass mode with perfusate comprising nutrient at the stated concentration in modified Krebs–Henseleit buffer (KHB) containing (mM): NaCl 120, KCl 4.5, $MgSO_4$ 1.0, Na_2HPO_4 1.8, NaH_2PO_4 0.2, $CaCl_2$ 1.25 and $NaHCO_3$ 25; gassed (19 : 1, O_2–CO_2) to pH 7.4 before use. [^{3}H]Inulin (0.70 kBq ml^{-1}) was also added for the determination of water fluxes. The flow rate of perfusate was 0.37 ml min^{-1} and that of gas 0.19 ml min^{-1}. To test the effect of drugs or artificial sweeteners on glucose absorption, or to resolve the contributions of SGLT1 and GLUT2 to glucose absorption by selective inhibition of GLUT2 with phloretin, the loop was perfused with glucose for a control period (usually 0–40 min) and then switched to perfusion with glucose and drug and/or sweetener for an experimental period (usually 40–90 min). Perfusions were viable over a period of 90 min. The control perfusate contained solvent vehicle to match the experimental period; the concentration of solvent (ethanol or DMSO) used for drugs or phloretin ranged from 0.1 to 0.3% v/v and solvent alone had no effect on any components of absorption. Glucose concentration was determined as the rate of loss from the luminal perfusate expressed in μmol min^{-1} (g dry weight)$^{-1}$. All procedures used conformed to the UK Animals (Scientific Procedures) Act 1986 and had the approval of the local Research Ethics Committee.

Apical membrane vesicles and Western blotting

Vesicles were prepared by modification of the method of (Corpe *et al.* 1996) with extensive precautions to maintain the *in vivo* integrity and localization of proteins, including protection of phosphorylation status (Mace *et al.* 2007). Briefly, trafficking of GLUT2 was arrested by flushing the loop with ice-cold buffered mannitol (20 mM imidazole buffer, pH 7.5, containing 250 mM mannitol) to which PMSF (0.1 mM) and a protease inhibitor cocktail (Sigma P-8340) were added. The phosphorylation status of the proteins was maintained by addition of 10 mM EDTA, 200 mM activated sodium orthovanadate, 20 mM NaF, 10 mM EGTA and 5 mM EDTA to the homogenization buffer. The loop was opened longitudinally on an ice-cold glass plate; mucosal scrapings were collected with an ice-cold glass microscope slide and immediately homogenized at 4°C in buffered mannitol using a Kinematica Polytron homogeniser (four 30 s bursts using the large probe at setting 7). Sucrase enrichment in vesicles ranged from 16- to 20-fold. There was no significant enrichment of Na^+–K^+-ATPase activity.

For Western blots, protein was separated by 10% SDS-PAGE, transblotted onto Polyvinylidene fluoride membrane (PVDF), probed with primary antibody and detected by Enhanced Chemiluminescence (ECL) (Helliwell & Kellett, 2002). Quantification of Western blots was performed using a Flowgen AlphaImager 1200 analysis system (Alpha Innotech Corporation, CA, USA). The levels of a given protein determined in vesicle preparations from jejunum at either 75 mM glucose or at 20 mM glucose + 1 mM sucralose were expressed relative to those in control preparations at 20 mM glucose

alone. The linear range of intensity response in ECL photographs was established using a 20-fold range of the amount of an actin standard (2–40 μg). After background correction, the response was linear (correlation coefficient, 0.996) for integrated density values ranging from 13 024 to 465 029. As far as possible, exposures for measurement of relative protein amounts were such that the intensity values fell within the middle part of the linear response range. The same loading of 20 μg protein was used for all samples: comparison of the relative levels of a given protein was made on a total protein basis in order to minimize potential complications that might be caused by the trafficking of other proteins in response to the same stimuli that affect trafficking of the given protein (Helliwell & Kellett, 2002).

Immunocytochemistry

Jejunum perfused with sugar or artificial sweetener for 30 min was fixed *in vivo* for 15 min with paraformaldehyde lysine periodate fixative (Affleck *et al.* 2003). Squares of tissue from the midpoint of the segment were incubated in fixative overnight, cryoprotected in 20% sucrose and embedded in OCT. Antigen was revealed by microwaving sections (7 μm) for 5–12 min, depending on antigen. Sections were blocked overnight, probed with primary antibody, washed and incubated with fluorophore-conjugated secondary antibody, washed again and mounted. For colocalization studies, dual staining for all combinations of any two proteins was undertaken utilizing primary antibodies raised in rabbit. For this reason, the antibodies were applied sequentially with antibody against protein 1 added, followed by the Alexa 488-conjugated secondary antibody. The sample was then extensively washed, re-blocked and the process repeated for protein 2 with Alexa 568-conjugated secondary antibody. Fluorescence micrographs were taken using a Zeiss LSM 510 META confocal microscope on an Axioplan 2 using a PlanApochromat 40 ×/1.3 or a 63 ×/1.4 lens (Carl Zeiss GmbH). Because of significant levels of broad autofluorescence in fixed and VectaShield-mounted sections of intestine, it was essential to use spectral unmixing to separate the fluorescent probes from the background signals. Emission profiles were recorded using unlabelled samples for autofluorescent profiles, and single-labelled specimens for Alexa 488 and 568 emission profiles. The localization of the two proteins was then separated into two channels, and autofluorescence into a separate image channel by linear unmixing using the referenced spectral profiles. Control samples included unlabelled, single-labelled (primary and secondary stained), and single primary labelled samples with both secondary antibodies used. In each case, these images were unmixed using the spectral profiles used for dual stained images, which exhibited no false assignment into the designated protein channels. The entire control procedure was repeated if any conditions were modified. λ subtraction on the different controls also established the efficacy of washing between sequential labelling with different antibodies raised in the same species. Specific staining was eliminated by preincubation of antibody with excess antigenic peptide in all cases where peptide was available (see below); as noted, any remaining background signals were automatically subtracted during spectral unmixing. In order to produce images with a differential interference contrast (DIC) overlay, conventional confocal microscopy without spectral unmixing was used, so that the merged and DIC overlay images could be easily generated to demonstrate morphological localization. For λ subtraction and spectral unmixing, the confocal microscope uses a different set of detectors, so that a DIC overlay cannot be readily generated.

Antibodies

Primary polyclonal antibodies were raised in rabbit to the following sequences. GLUT2: residues 40–55 SHYRHVLGVPLDDRRA in the first extracellular loop of rat GLUT2 (commissioned from Research Genetics, U.S.A). The antibody was affinity-purified according to the manufacturer's instructions using a Pierce (USA) SulfoLink Kit. SGLT1: residues 564–575 RNSTEERIDDLDA of rat SGLT1 (commissioned from Research Genetics). Taste receptors: N-terminal extracellular region of T1R1 (ab12676) and T1R3 (ab12677) from Abcam, UK; C-terminal region of T1R2 (Chemicon International, USA, AB5626P). Transducin α: residues 344–353 CKENLKDCGLF (ab19427) from Abcam. α-gustducin: highly divergent domain of $G_{\alpha gust}$ of rat origin, sc-395. PLC β2: C-terminal region, sc-206. For Western blotting, affinity-purified antibodies were used at 1 : 100 dilution for taste receptors and transducin, and 1 : 500 for *a*-gustducin and PLC β2. The secondary antibody was goat anti-rabbit IgG conjugated with horseradish peroxidase (Sigma A0545) used at 1 : 5000 dilution. For immunocytochemistry, primary antibody dilutions were 1 : 100 for taste receptors, 1 : 200 for G-proteins and 1 : 500 for PLC β2. Goat anti-rabbit secondary antibodies Alexa 488 and 568 (Invitrogen) were used at 1 : 500. In order to confirm specificity of labelling, some blots or sections were treated with antibody that had been neutralized by incubation for 1 h with excess antigenic peptide (antibody to peptide 1 : 1 v/v, peptide 50 μg ml^{-1}).

Materials

Acesulfame potassium and 2,3-dihydro-1,2-benzoisothiazol-3-one-1,1-dioxide (saccharin) were from

Fluka Chemie GmbH. 1,6-dichloro-1,6-dideoxy-β-D-fructofuranosyl-4-chloro-4-deoxy-α-D-galactopy-ranoside (sucralose) was a gift from Tate and Lyle (McNeil Nutritionals, LLC). U-73122, an inhibitor of G-protein-mediated activation of PLC, was from Sigma, UK.

Statistical analysis

Values are presented as means ± S.E.M. and were tested for significance using paired or unpaired Student's *t* test.

Results

To determine whether intestine contains a functional sweet taste reception system that regulates the apical GLUT2 pathway, we investigated the effect of sucralose (1 mM) on the absorption of glucose (20 mM) in perfused rat jejunum *in vivo*. Sucralose is not absorbed and not metabolised and thought to act only through T1R2 + T1R3; at 1 mM, it invokes the maximal Ca^{2+} response by lingual taste receptors (Li *et al.* 2002). At 20 mM glucose, there is a basal level of GLUT2 in the apical membrane; rapid glucose-induced insertion of apical GLUT2 is first detectable at 30 mM glucose. Use of 20 mM glucose should therefore permit ready detection of any effect of sucralose on apical GLUT2. The results were compared with those for 75 mM glucose alone, for which there is substantial apical GLUT2 insertion above the basal level. The apical GLUT2 and SGLT1 components were resolved by the use of phloretin, which inhibits apical GLUT2 but not SGLT1 in whole intestine (Kellett & Helliwell, 2000).

Rat jejunum was perfused with 20 mM glucose for 30 min to determine the initial control rate (Fig. 1*A*, triangles), after which the perfusate was switched to one containing 20 mM glucose and 1 mM sucralose (Fig. 1*A*, S arrowhead); after a lag, the rate of absorption doubled. With 20 mM glucose alone (Fig. 1*A*, squares), phloretin introduced into the perfusate at 40 min (Fig. 1*A*, P arrowhead) resulted in rapid inhibition of absorption to give a new steady-state: the phloretin-sensitive apical GLUT2 component accounted for 41% of the total rate and phloretin-insensitive component was attributed to SGLT1 (see arrows for the 20 mM control C in Fig. 1*A*). When perfused with glucose and sucralose from the start (Fig. 1*A*, circles), there was a prolonged up-regulation in which the rate of glucose absorption doubled between 5 and 20 min. Such up-regulation is not seen with 20 mM glucose alone, but is seen with 75 mM glucose, where it is identified with apical GLUT2 insertion (Kellett & Helliwell, 2000). Sucralose had little effect on the phloretin-insensitive SGLT1 component. Thus sucralose selectively increased the apical GLUT2 component 3.2-fold (compare arrows for C and +S). Western blotting and immunocytochemistry revealed that the increase correlated with a 3.4-fold increase in apical GLUT2, similar to the 3.7-fold increase for 75 mM compared with 20 mM glucose (Figs 2 and 3, and Table 1). Neither sucralose nor 75 mM glucose had a significant effect on the levels of SGLT1 at the apical membrane compared with the effect of 20 mM glucose (Figs 2 and 3, and Table 1; see also Discussion). Perfusion with different concentrations of sucralose in the absence and presence of phloretin gave the K_a of sucralose for the apical GLUT2 component as approximately 0.1 mM (Fig. 1*B*).

The involvement of PLC β2 in the signalling pathway was demonstrated by perfusion with U-73122 (U), an inhibitor of G-protein-coupled PLC β2 activation, and the use of phloretin (P) to determine the apical GLUT2 and SGLT1 components. As before, the perfusions were split into two periods for each test condition, 0–40 min for a given condition and 40–80 min to determine the effect of an inhibitor on that condition. In Fig. 1*C*, the middle pair of bars show the rate of absorption of 20 mM glucose in the absence (C, open bar) and presence of 10 μM U-73122 (C + U, hatched bar); U-73122 had no effect on total absorption. The left-hand pair of bars show the rate of absorption of 20 mM glucose in the absence (C, open bar) and presence of phloretin (C + P). The right-hand pair of bars show the rate of absorption of 20 mM glucose plus U-73122 in the absence (C + U, open bar) and presence of phloretin (C + U + P); comparison of the right- and left-hand pairs shows that U-73122 had no effect on either the phloretin-sensitive basal apical GLUT2 component or the phloretin-insensitive SGLT1 component of absorption at 20 mM glucose. Figure 1*D*, in which C represents 20 mM glucose plus 1 mM sucralose, shows that U-73122 selectively inhibited stimulation of apical GLUT2-mediated absorption by sucralose. Moreover, Fig. 1*E*, in which C represents 75 mM glucose, shows that U-73122 also selectively inhibited the stimulation of the apical GLUT2 component by high glucose concentration. As the absorption rate of 75 mM glucose was the same in the absence and presence of sucralose (37.9 ± 2.0 and 41.4 ± 1.4 μmol min^{-1} (g dry weight)$^{-1}$, respectively, $n = 4$ each), these data show that glucose at high concentrations and sucralose at low glucose concentrations act through the same PLC β2-dependent signalling pathway.

Activation of PLC β2 in cells by taste receptors results in increases in cytosolic Ca^{2+} concentration. When rat T1R2 + T1R3 receptors are co-expressed in HEK-293T cells, the maximal cytosolic Ca^{2+} concentration induced by saccharin is about one-third that induced by acesulfame potassium or sucralose (Li *et al.* 2002). Accordingly, Fig. 1*F* shows that in perfusions with 20 mM glucose (C), acesulfame potassium (K) increases the apical GLUT2 component to the same extent as sucralose (S), whereas saccharin (Sa) increases it by only one-fifth ($P = 0.02$).

The presence of taste reception signalling components was identified by Western blotting of apical membrane vesicles. Figure 2 shows the full Western blots for three different preparations in each condition for perfusion with 75 mM glucose, 20 mM glucose and 20 mM glucose + 1 mM sucralose. GLUT2 presents as a single band at 63 kDa; there is no evidence of any other species. SGLT1 presents as a tight doublet, which appears as a single broad band at 75 kDa, with no evidence of any other species. However, signalling components, especially transduction proteins and downstream targets, show a different pattern from transporters, presenting with bands of both lower and higher molecular weight than the native protein. Such bands can arise as a result of simultaneous cleavage and turnover on activation. Indeed, we have already described in detail one such mechanism,

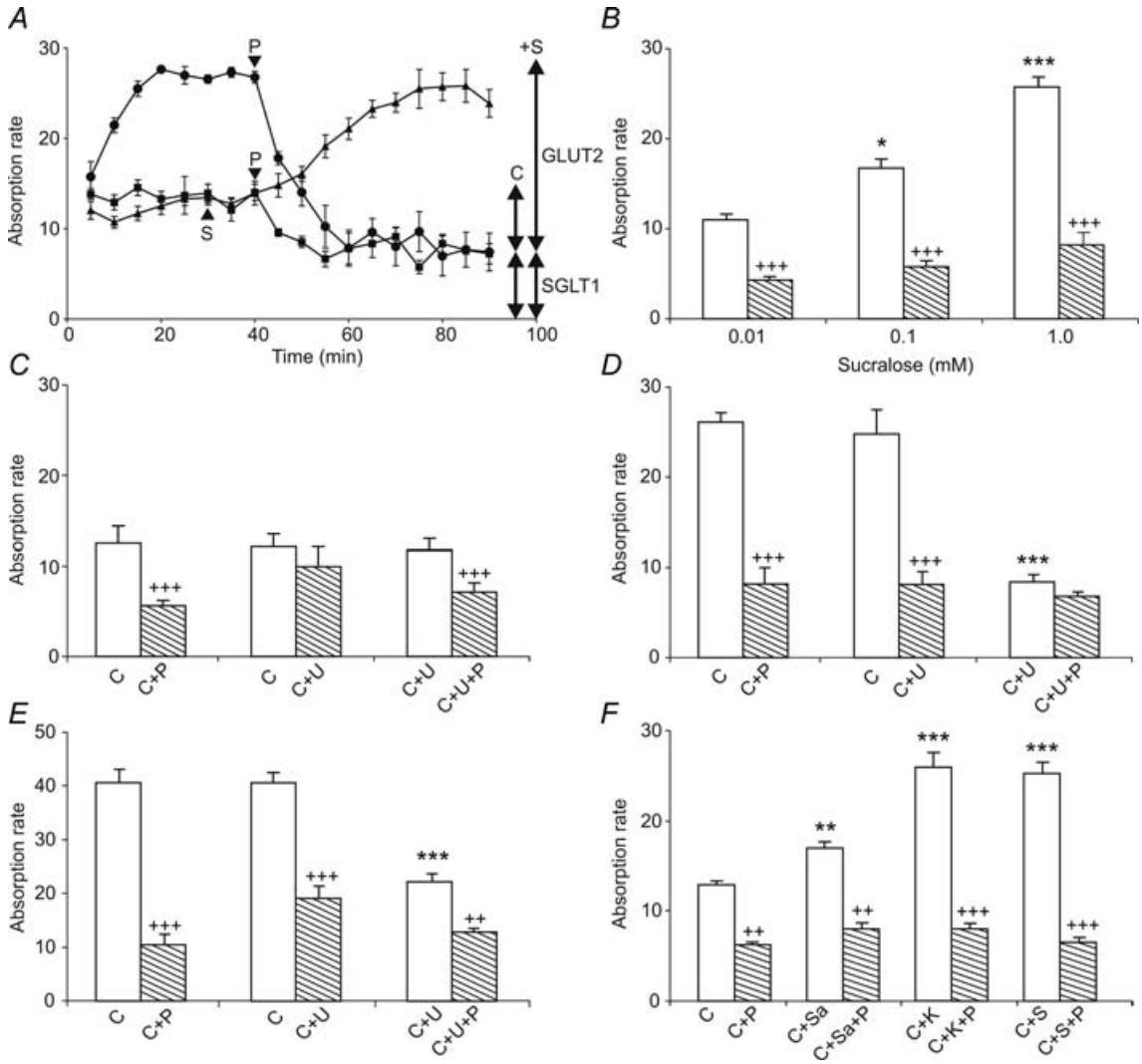

Figure 1. Artificial sweeteners and glucose stimulate glucose absorption
A, effect on 20 mM glucose absorption of sucralose (▲, 1 mM, S arrowhead) added at 30 min and of phloretin added at 40 min (■, 1 mM P arrowhead): effect on sucralose-stimulated glucose absorption (0–40 min) of phloretin added at 40 min (●). *B*, concentration dependence of stimulation of glucose absorption by sucralose; 20 mM glucose and sucralose were perfused in the absence (□, 0–40 min) and presence (▩, 40–80 min) of 1 mM phloretin. *C–E*, role of PLC β2 for (*C*) 20 mM glucose (C), (*D*) 20 mM glucose + 1 mM sucralose (C) and (*E*) 75 mM glucose (C); open bar perfusion for 0–40 min *versus* hatched bar for 40–80 min; U, 10 μM U-73122; P, 1 mM phloretin. *F*, comparison of effects of sucralose (S), acesulfame potassium (K) and saccharin (Sa) on the components of 20 mM glucose absorption (C) determined after addition of phloretin (P) at 40 min. Absorption rate in μmol min^{-1} (g dry weight)$^{-1}$; values are means ± S.E.M, $n = 4$–6 for each condition. Student's *t* test: unpaired comparison for different perfusions, open bar for experiment with open bar for control (C only): $^{*}P < 0.05$, $^{**}P < 0.01$, $^{***}P < 0.001$, paired comparison within the same perfusion; hatched bar with adjoining open bar, $+P < 0.05$, $++P < 0.01$, $+++P < 0.001$.

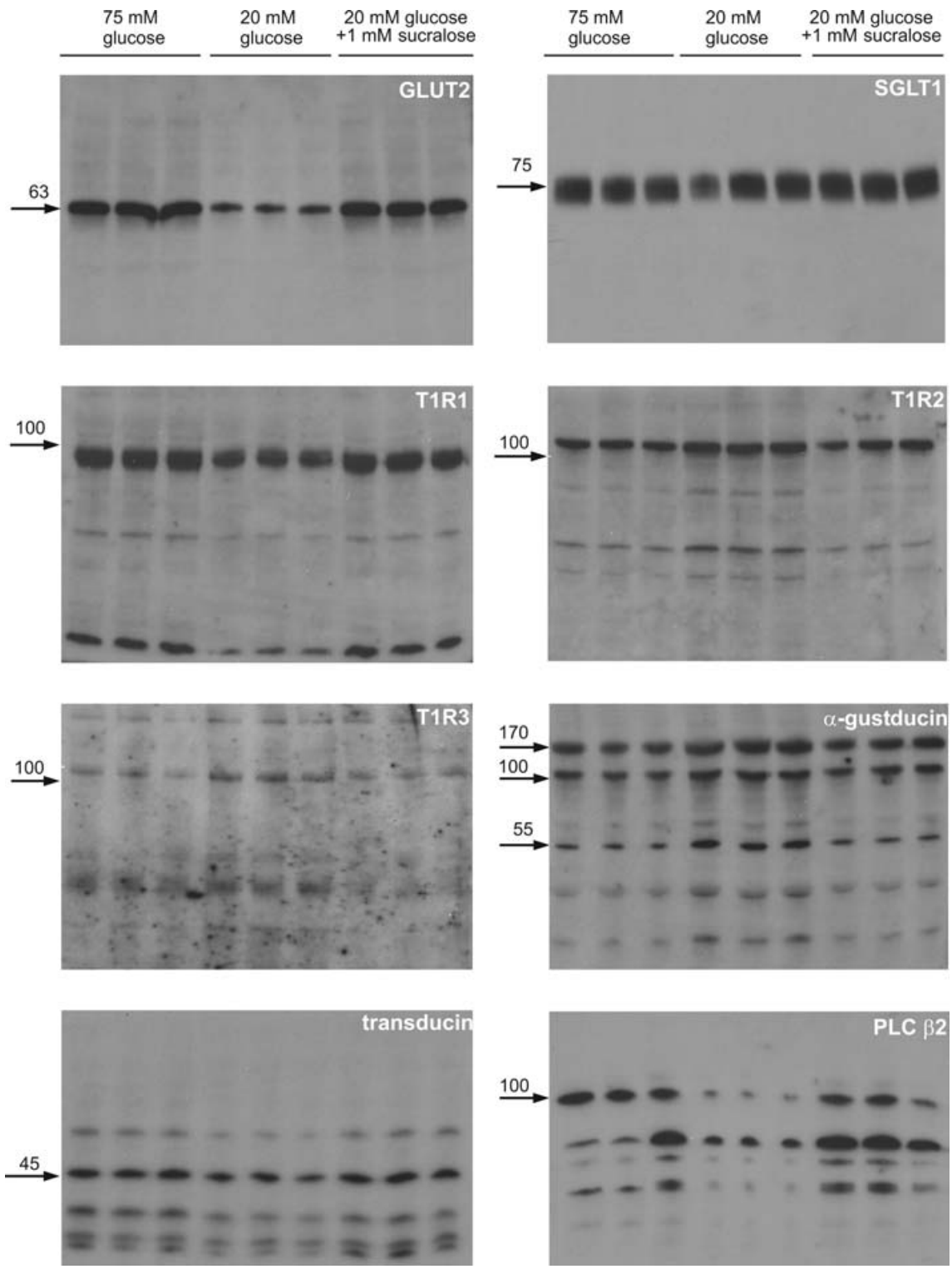

Figure 2. Regulation of transporters and taste reception signalling components by glucose and sucralose detected in Western blots of apical membrane vesicles

Apical membrane vesicles were prepared from rat jejunum perfused *in vivo* for 20 min with 75 mM glucose, 20 mM glucose or 20 mM glucose + 1 mM sucralose. Vesicle protein (20 μg) was then separated by SDS-PAGE (10% gels), transblotted on to PVDF and Western blotted for signalling components. All bands for a given protein were abolished by preincubation of antibody with excess cognate peptide; peptides were not available for T1R1 and T1R3 (data not shown).

Table 1. Band intensities in Western blots relative to those at 20 mM glucose

	75 mM glucose	20 mM glucose	20 mM glucose + 1 mM sucralose
GLUT2	$3.70 \pm 0.12^{***}$	1.00 ± 0.07	$3.35 \pm 0.03^{***}$
SGLT1	1.28 ± 0.28^{NS}	1.00 ± 0.28	1.35 ± 0.21^{NS}
T1R1	$1.76 \pm 0.05^{***}$	1.00 ± 0.04	$1.56 \pm 0.05^{**}$
T1R2	$0.60 \pm 0.03^{**}$	1.00 ± 0.03	$0.56 \pm 0.27^{*}$
T1R3	$0.51 \pm 0.16^{***}$	1.00 ± 0.04	$0.45 \pm 0.24^{**}$
55 kDa α-gustducin	$0.24 \pm 0.03^{***}$	1.00 ± 0.03	$0.36 \pm 0.07^{***}$
45 kDa transducin	$1.88 \pm 0.20^{*}$	1.00 ± 0.12	$2.36 \pm 0.09^{**}$
100 kDa PLC β2	$14.82 \pm 2.24^{**}$	1.00 ± 0.23	$12.23 \pm 0.20^{**}$

$^{*}P < 0.05$; $^{**}P < 0.01$; $^{***}P < 0.001$; NS, not significant.

namely the rapid glucose-induced activation of PKC βII on which apical GLUT2 insertion depends (Kellett & Helliwell, 2000). Activation of PKC βII is initiated by translocation of the native 80 kDa protein from cytosol to the apical membrane, where it undergoes calpain-dependent cleavage to a phosphorylated, 49 kDa active species. The latter is then dephosphorylated to a 42 kDa inactive species, which is targeted for rapid turnover and degradation by polyubiquitylation to produce a series of species of 180 and > 250 kDa (Helliwell *et al.* 2003).

T1R1, T1R2 and T1R3 all show some evidence of proteolysis in these preparations from perfused jejunum; indeed, it was particularly hard to obtain a satisfactory blot for T1R3. The difficulty did not arise from the particular antibody used, because immunocytochemistry worked reasonably well. We took considerable precautions to maintain protein integrity during isolation and found that, in addition to a standard cocktail of protease inhibitors, general control of the phosphorylation state appeared to be helpful. Whether the proteolysis is an inherent part of the signalling process or simply represents exceptional sensitivity of the receptors to endogenous proteases during preparation is not clear.

α-gustducin displays strong bands at 110 and 170 kDa and a lighter, but clear band at 55 kDa,

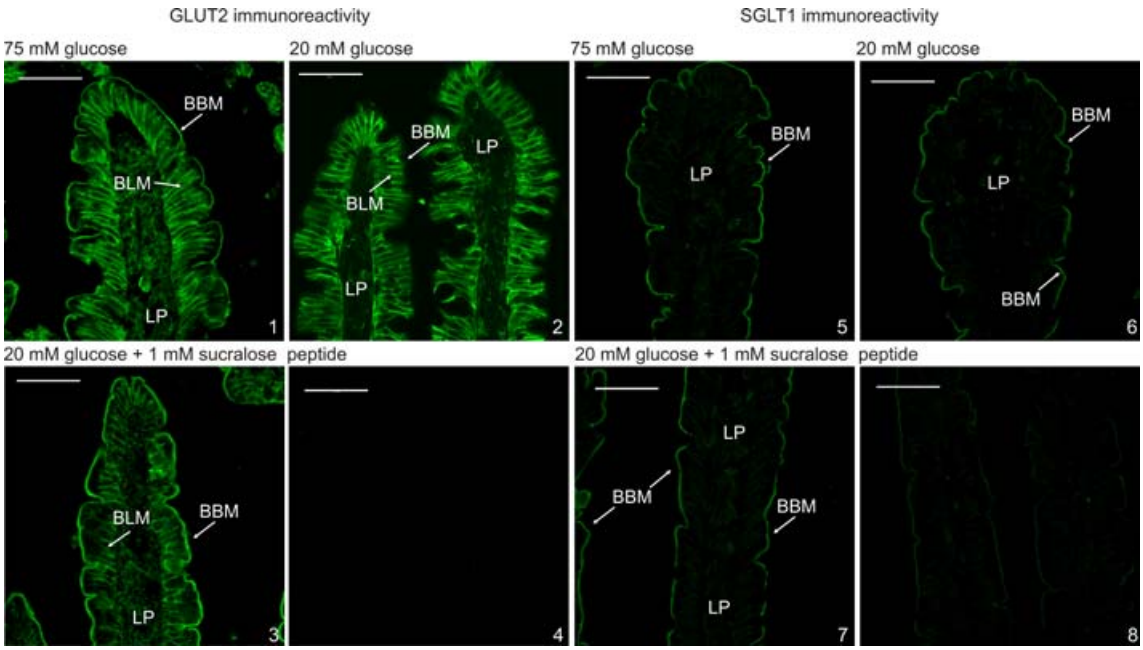

Figure 3. Immunocytochemistry of the regulation of apical GLUT2 and SGLT1
Extracellular loop antibody was used to detect apical GLUT2 in the brush-border (BBM) and basolateral (BLM) membranes of perfused rat jejunum using fluorescein isothiocyanate (FITC)-conjugated secondary antibody. Apical GLUT2 was increased at 75 mM glucose and by sucralose at 20 mM glucose compared with 20 mM glucose alone. There was no significant alteration of SGLT1 between the different conditions. Both peptide controls were performed with vesicles prepared at 75 mM glucose. LP, lamina propria.

corresponding to the native molecular weight; there is some evidence of limited proteolysis. The lighter 55 and stronger 110 kDa bands have already been reported for unperfused mouse intestine (Dyer *et al.* 2005). In principle, the 110 and 170 kDa bands could represent multimers of the native species at 55 kDa. However, an alternative explanation is that the higher molecular weight bands represent ubiquitylated species resulting from sugar-induced activation of α-gustducin. Indeed such rapid ubiquitylation occurs for rhodopsin and rod transducin in response to light with the production of multiple bands of 50 to $>$ 200 kDa representing mono- to polyubiquitylated species (Obin *et al.* 1996). The major band for intestinal transducin appears at its native molecular weight of 45 kDa, but again minor higher and minor lower molecular weight bands are seen. Agonist-induced activation of PLC β isoforms involves calpain-dependent cleavage of the native enzyme (Banno *et al.* 1994); indeed, cleavage of the intestinal enzyme is so effective that several bands are produced by further rapid proteolysis and most probably turnover. For GLUT2, SGLT1, T1R2, α-gustducin, transducin and PLC β2, preincubation of antibody with excess cognate peptide abolished all bands for that protein, confirming the specificity of detection (data not shown). For T1R1 and T1R3, no peptide was available, because the sequence was deemed 'commercially sensitive'. However, the fact that blots and immunocytochemistry gave consistent results for the apical membrane indicates that labelling is specific. As our extensive studies with PKC βII illustrate, elucidation of the detailed mechanism of activation and turnover for each protein is beyond the scope of the present paper.

Table 1 presents the changes in relative band intensities, for each band of particular interest the mean intensity from three preparations for each condition is expressed relative to that at 20 mM glucose taken as 1.00. For any given protein, the bands in Table 1 show the same relative changes between 75 mM, 20 mM and 20 mM + sucralose as all other bands for that protein; the one exception is PLC β2, where the initial 100 kDa species appears to be turned over so rapidly that precise timing with respect to perfusion and/or preparation would be very difficult to achieve. From the blots and Table 1, it is apparent that T1R2, T1R3 and α-gustducin traffic away from the membrane in response to high glucose or sucralose at low glucose concentration; in contrast T1R1, transducin and PLC β2 traffic to the membrane. Rapid trafficking of signalling components to and from the apical membrane and rapid turnover of transduction and downstream targets in response to sugars appears to be an essential feature of the regulation of the intestinal taste receptor system.

Immunocytochemistry identified Paneth cells, SCCs and enterocytes as sites of taste reception components. Images 1–4 of Fig. 4 show the T1R1 (green) and T1R3 (red) split images, together with the differential

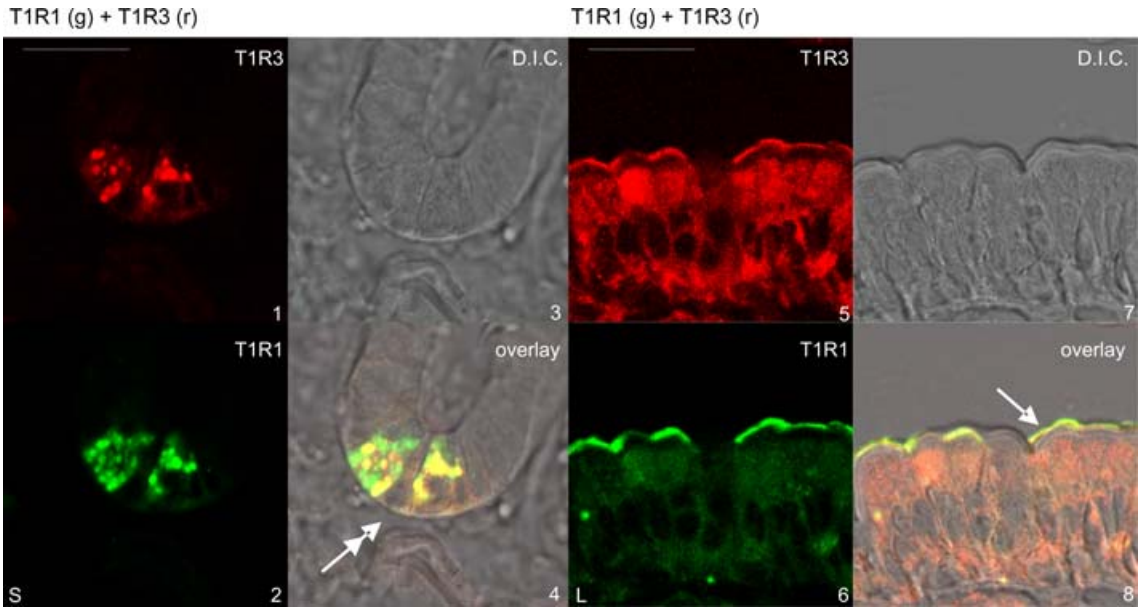

Figure 4. Demonstration of the localization of taste receptors in Paneth cells and in enterocyte apical membrane
T1R1 in green (g), T1R3 in red (r), differential interference contrast (DIC). Double-headed arrow, Paneth cells; single-headed arrow, brush-border membrane. L, low 20 mM glucose; S, 20 mM glucose + 1 mM sucralose. Scale bar, 50 μm. Note that these images were not taken using spectral unmixing, so that DIC images could be used to confirm localization (see Methods).

interference contrast (DIC) image of the crypts; the images were obtained by conventional confocal microscopy, that is without spectral unmixing, in order to facilitate the generation of a merged DIC overlay (see Methods). The overlay confirms the colocalization of T1R1 and T1R3 in the secretory granules of the Paneth cells at the very bottom of the crypts (Porter *et al.* 2002). Localization of the secretory granules of the Paneth cells shown in Fig. 5 by spectral unmixing is confirmed by reference to Fig. 4. Strong Paneth cell labelling was seen regularly, but not in every crypt (Fig. 5, images 1–4). T1R1 and T1R3 were routinely colocalized with transducin and, much less frequently, with α-gustducin (Fig. 5, images 1–4). Different secretory granules had different proportions of taste reception components, as indicated by gradation of colours from red through yellow to green. T1R2 was not seen in Paneth cells, but was observed in the brush-border of crypts (Fig. 5, image 9); PLC β2 was not seen in secretory granules, but significant cytosolic labelling was often seen in Paneth cells. Gustducin was widespread throughout the crypts in cytosol, but transducin less so. Specificity of labelling was confirmed by preincubation of antibody with excess cognate peptide in all cases where peptide was available (data not shown); peptide was not available for T1R1 and T1R3. In addition, secretory granules in Paneth cells were not labelled with any of the transporter antibodies that we regularly use (i.e. SGLT1, C-terminal GLUT2, extracellular loop GLUT2, GLUT5 and PepT1), or indeed with T1R2.

In SCCs in villi (Fig. 5), strong punctuate labelling of T1R2 was seen routinely and was colocalized with high (Fig. 5, image 5) or very low levels (Fig. 5, image 6) of

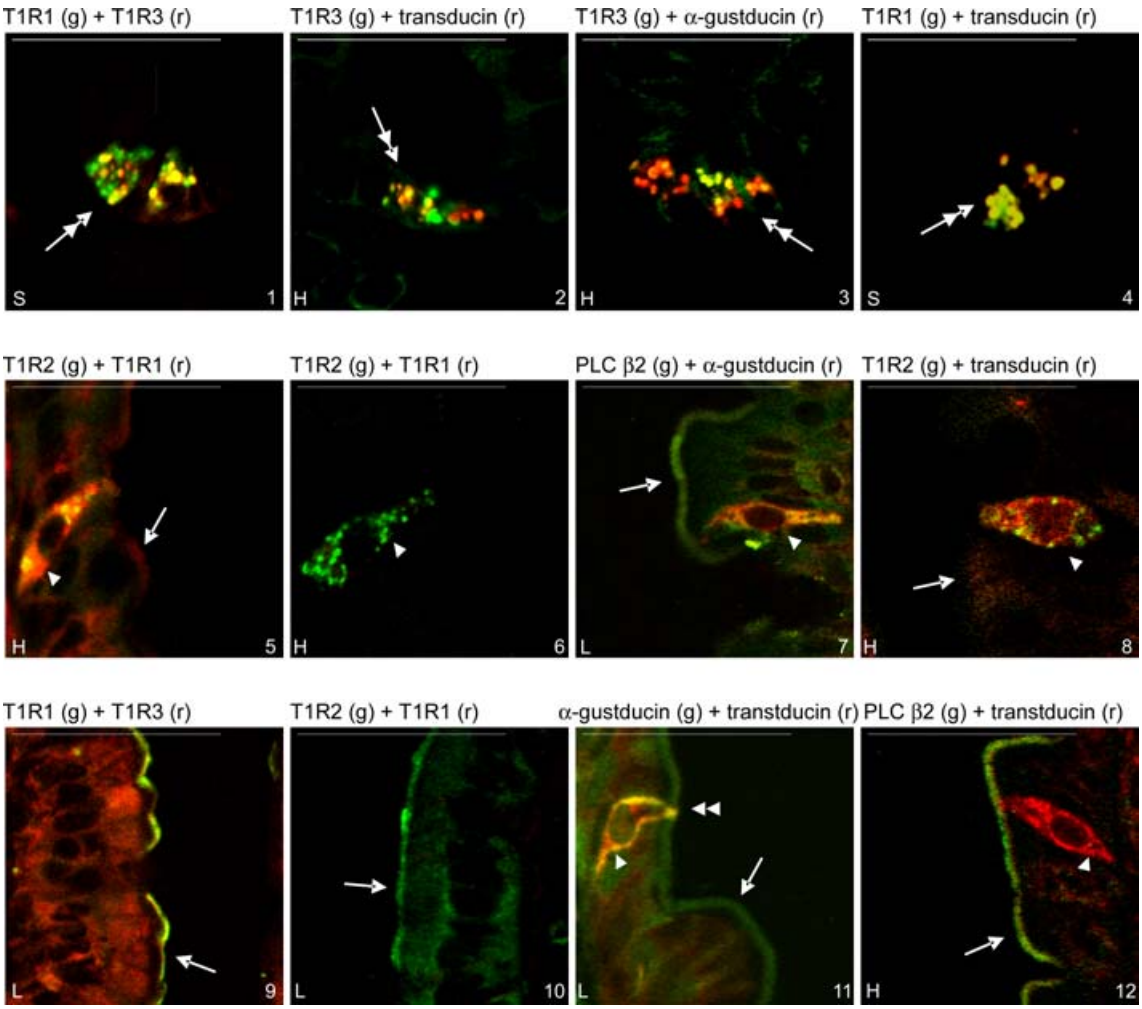

Figure 5. Colocalization of taste reception signalling components in rat jejunum
Double-headed arrow, Paneth cells located at the very bottom of the crypt as shown in image 4 of Figure 4; single-headed arrow, brush-border membrane; single arrow-head, chemosensory cells (SCCs); double arrow-head, SCC tip in brush-border membrane. Colour labelling: green, g; red, r. H, high 75 mM glucose; L, low 20 mM glucose; S, 20 mM glucose + 1 mM sucralose. Scale bar, 50 μm. Localization of images 1–4 is made by reference to the overlay image in Figure 4 (see text and Methods).

T1R1. We have not observed T1R3 in SCCs in rat jejunum, but it has been observed in a subset of transient receptor potential melastatin family member 5 (Trpm5)-expressing SCCs in mouse (Bezencon *et al.* 2007). Gustducin, transducin and PLC β2 were widespread in SCCs (Fig. 5, images 7, 8, 11 and 12) and clearly showed the bipolar structure identified by Sbarbati & Osculati (2005). Gustducin was normally colocalized with transducin (Fig. 5, image 11); the latter, however, was sometimes seen alone (Fig. 5, image 12). PLC β2 was colocalized with α-gustducin and transducin in SCCs (Fig. 5, images 7 and 12). There are at least 15 SCC subtypes, comprising about 0.06% in total of all intestinal cells. Like taste buds, different SCC subtypes clearly contain different combinations of sensing components, but the presence of so many SCC subtypes with variable distributions precluded quantitative analysis.

Figure 6 illustrates the factors which have to be taken into account in order to analyse cytosolic and apical membrane labelling. The spectral analysis shows colocalization of α-gustducin (green) and transducin (red) labelling. The right-hand image shows two adjoining villi; note that some cells are largely green in colour, whereas others are largely orange/brown, indicating considerable variability in the cytosolic levels and colocalization of α-gustducin and transducin. The left-hand spectrum is the λ spectrum comprising all spectral contributions including autofluorescence and reflection (peak at λ560 nm); note that autofluorescence, reflection and unassigned residuals are automatically subtracted when the spectra are unmixed to provide the images in Figs 4 and 5. The red cross is over an SCC in which α-gustducin and transducin are colocalized. This corresponds to the red line spectrum with peaks at λ523 (α-gustducin, green labelling) and λ605 (transducin, red labelling) at an intensity value just under 3000. The green line spectrum reflects that detected at the green cross, which was chosen to be in an area of cytosol in which both α-gustducin and transducin were present. The blue line spectrum corresponds to the apical membrane at the blue cross, while the yellow line is background. Detailed quantification is impossible because of the variability of the distributions of α-gustducin and transducin, but a rough average over just three such spectra suggests that the signal from α-gustducin in an SCC is about 3-fold greater than that in cytosol and 9-fold greater than that in the apical membrane. We therefore found that any attempt to reduce image background excessively in order to highlight SCCs, because of their similarity to taste cells, resulted in the loss of much essential information in enterocyte cytosol and brush-border; such information is most probably related to the regulation of sugar absorption. The Western blots and extensive immunocytochemical controls validate the apical membrane labelling.

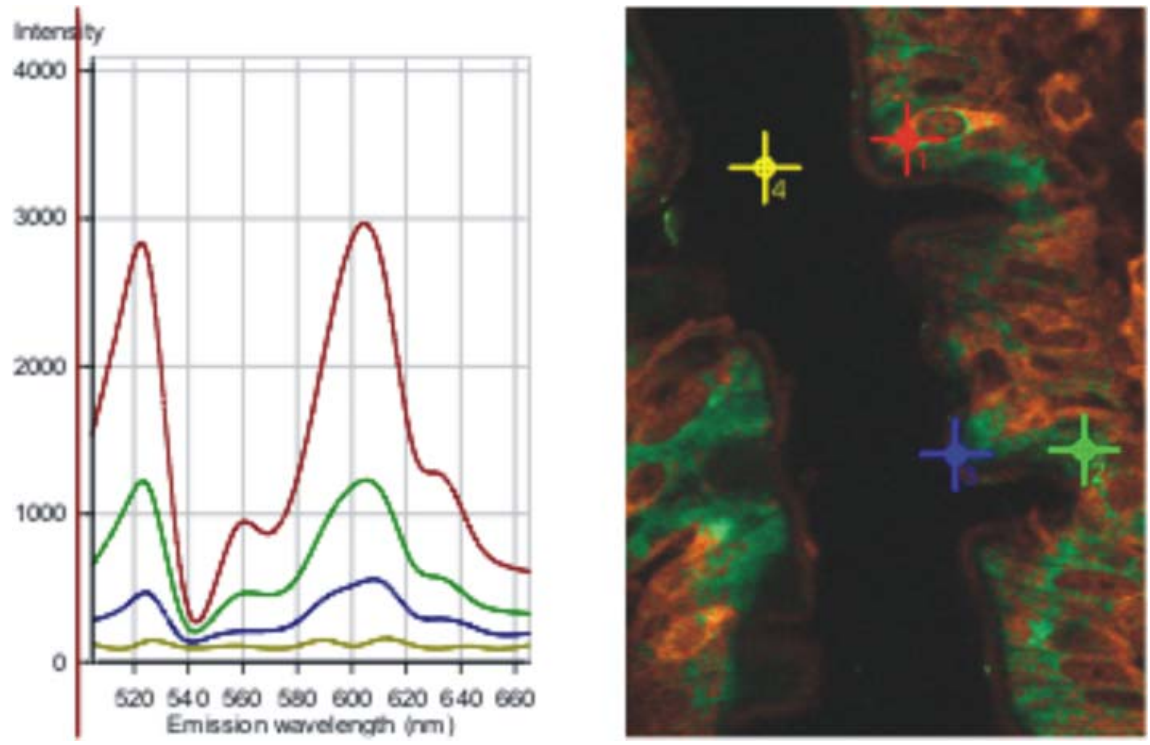

Figure 6. Spectral analysis of the cytosolic and apical membrane colocalization of *a*-gustducin and transducin
The section was prepared from jejunum perfused with 75 mM glucose. See text for detailed explanation.

T1R1, T1R2, T1R3, *a*-gustducin, transducin and PLC $\beta 2$ are all present in the apical membrane and cytosol of enterocytes. Images 5–8 in Fig. 4 show a typical red–green split and DIC overlay for T1R1 and T1R3 colocalization (see also image 9 in Fig. 5). T1R1 is also colocalized with T1R2, although the levels of each are quite variable within and between villi (Fig. 5, images 10–12). The cytosolic and apical levels of T1R receptors are about one-third of those in SCCs (data not shown). Our conclusions here agree well with the report that lingual T1R receptors are predominantly localized intracellularly (Li *et al.* 2002). Moreover, the clonal enterocytic Caco-2 cell line contains transcripts for T1R3 and α-gustducin (E. Brot-Laroche, personal communication).

Discussion

The data reveal that the apical GLUT2 component of intestinal glucose absorption is induced by the sensing of glucose itself at high concentrations; 75 mM glucose causes rapid apical GLUT2 insertion, whereas 20 mM does not. There are six reasons to believe sensing occurs through sweet taste receptors. (i) Artificial sweeteners, which are not absorbed and not metabolized, strongly stimulate glucose absorption at 20 mM by rapid insertion of apical GLUT2; the only way they can therefore act is through a receptor with the appropriate properties. (ii) The simple sugar glucose acts in the range 30–100 mM glucose to insert apical GLUT2, whereas artificial sweeteners act at 1–2 mM, as seen for the T1R2 + T1R3 sweet taste receptor heterodimer expressed heterologously. (iii) Both glucose and sucralose act through a PLC $\beta 2$-dependent signalling system, which is G-protein dependent, and is one of the established signalling systems for sweet taste receptors. (iv) The ability of different artificial sweeteners to enhance the apical GLUT2 component of absorption parallels their maximal potencies in enhancing intracellular Ca^{2+} concentration in a heterologous expression system, with sucralose > acesulfame potassium $\approx$ saccharin. (v) The pattern of rapid apical membrane trafficking of GLUT2 and the taste reception system signalling components induced by high glucose is the same as that induced at low glucose concentration by sucralose. (vi) The classic sweet taste receptor components, T1R2 + T1R3 and α-gustducin, all decrease in response to sweeteners, suggesting that internalization may be necessary to signal to increase apical GLUT2. By contrast, the classic amino acid taste receptor components, T1R1 and transducin, and also PLCβ_2 and behave reciprocally. The fact that the amino acid taste receptor is regulated by sweeteners is itself remarkable, suggesting that the sensing mechanism acts to strike a balance between sugars and amino acids, possibly by competition for the common subunit T1R3.

Sheep intestine expresses a sugar sensor, which stimulates SGLT1 synthesis by a cAMP- and G-protein-dependent pathway: infusion of ruminant sheep intestine with a membrane impermeable D-glucose analogue first results in detection of SGLT1 after 3 h (Dyer *et al.* 2003). We have not found any receptor/sensor-mediated change in either the apical level of SGLT1 or in the magnitude of SGLT1-mediated absorption. However, this is not surprising, because induction of SGLT1 synthesis cannot be detected on the timescale of our perfusions. Thus it takes no more than 15–20 min to achieve a steady state of absorption at high glucose concentrations or with sucralose at low glucose concentrations; all vesicle preparations are made after 30 min perfusion. By contrast, SGLT1 synthesis takes place primarily in the crypts and lower villus in both sheep and rat and is not reprogrammed in higher villus regions (Ferraris, 2001). As a result, it takes 12–24 h to detect carbohydrate-induced SGLT1 synthesis in mouse or rat. The fact that synthesis of SGLT1 can be detected in sheep after just 3 h reflects the fact that SGLT1 in ruminant sheep increases 50- to 90-fold from a background of almost zero, whereas in rat SGLT1 increases only $\leq$ 2-fold. Exposure of intact rat jejunal mucosa to glucose up-regulates active glucose transport within 30 min (Sharp *et al.* 1996). Moreover, SGLT1 can clearly recycle to and from the apical membrane, as apical SGLT1 levels may be modulated within minutes by cholecystokinic (CCK-8) (Hirsh & Cheeseman, 1998). However, detailed investigation reveals that glucose-induced increases in SGLT1 activity occur without redistribution of cellular SGLT1 (Khoursandi *et al.* 2004). Apical GLUT2 is present in sheep fed a molasses-rich diet (JR Aschenbach, personal communication). Interestingly, as sweet taste receptors can signal through both cAMP and PLC $\beta 2$ (Margolskee, 2002), it seems they may regulate short-term events (minutes) through PLC $\beta 2$ and longer events (hours), such as SGLT1 synthesis, through cAMP.

The presence of key taste reception signalling components in different distributions at different strategic locations implies that Paneth cells, SCCs and enterocytes have distinct sensing roles. This conclusion is underlined by the fact that we have not seen T1R2 in the secretory granules of Paneth cells or T1R3 in SCCs. As noted, enterocytes have all the necessary components to account for the changes in absorption seen in response to high glucose concentration and sucralose. Paneth cells, which contain the amino acid taste receptor components, may be involved in the response to feeding after starvation (Ahonen & Penttila, 1975). Of note, T1R2 is present at the apical membrane of crypt cells, which is the site of SGLT1 synthesis. Furthermore, we have recently obtained one image of an SCC in crypts containing T1R2. It therefore seems that the sugar sensor documented in sheep may be T1R2. SCCs could perhaps be involved in regulation of

food intake, but what is the significance of the fact that T1R2 labelling is clearly punctuate, whereas T1R1 is not? Our conclusions are in accord with the suggestion of others that SCCs and enterocytes might have distinct sensing roles (Hofer *et al.* 1999). However, cross-talk between all three systems may exist and it is thought that NO may play such a role (Hofer *et al.* 1999). Other undiscovered taste receptors may yet be involved (Delay *et al.* 2006).

There has been great uncertainty about the concentrations of sugars generated at the apical membrane during the hydrolysis of digestion products or simple sugars such as disaccharides and α-limit dextrins; such concentrations have been viewed as key to the continuing debate on the likely contribution of active and facilitated/passive pathways to total glucose absorption. For rats on nearly physiological diets, average free glucose concentrations across the jejunal lumen range from 0.2 mM before a meal to 48 mM afterwards (Ferraris *et al.* 1990); these figures span the effective concentration range of SGLT1 activity and were taken to suggest that SGLT1 accounted for all absorption. By contrast, indirect measurements from the rate of membrane hydrolysis of maltose suggest that the effective local concentration generated at the surface of the apical membrane is of the order of 300 mM (Pappenheimer, 1993), which would provide the necessary gradient to drive a significant diffusive component. We observed that apical GLUT2 insertion was first detected at 30 mM and increased at 100 mM glucose (Kellett & Helliwell, 2000). When T1R2 and T1R3 are coexpressed in a stable G_α HEK-293 cell derivative, 30 and 100 mM sucrose correspond to 15% and 85%, respectively, of the maximal increase in intracellular Ca^{2+} concentration possible in response to sucrose (Li *et al.* 2002). Moreover, sucrose induces apical GLUT2 very effectively (Gouyon *et al.* 2003). If we assume that glucose and maltose induce the same response as sucrose, then the range of effective glucose concentrations at the apical membrane corresponds to 30–200 mM glucose. The presence of a natural sugar receptor at the apical membrane with properties that correspond so closely to apical GLUT2 induction implies that such effective local concentrations are routinely generated during digestion and thereby confirms that apical GLUT2 then provides a major pathway of intestinal glucose absorption.

High levels of glucose and fructose in processed food products are thought to be a significant factor in the current upsurge of obesity and diabetes in the Western world. Such insulin-resistant states are characterized by high levels of apical GLUT2 (Corpe *et al.* 1996); already, clinical trials are proposed to moderate excessive sugar absorption and insulin excursions by targeting apical GLUT2 with the polyphenol, quercetin, found in vegetables and red wine (Kwon *et al.* 2006). The food industry has moved to replace simple sugars partially with artificial sweeteners on the assumption that, because the latter are calorie-free, they are nutritionally inert. Our finding that artificial sweeteners signal to a major food-sensing system to increase the apical GLUT2 component of intestinal sugar absorption during the course of a meal shows this assumption no longer holds. Moreover, there are likely to be wide interactions between artificial sweeteners and important food constituents through apical GLUT2.

References

Adler E, Hoon MA, Mueller KL, Chandrashekar J, Ryba NJ & Zuker CS (2000). A novel family of mammalian taste receptors. *Cell* **100**, 693–702.

Affleck J, Helliwell PA & Kellett GL (2003). Immunocytochemical detection of GLUT2 at the rat intestinal brush-border membrane. *J Histochem Cytochem* **51**, 1567–1574.

Ahonen A & Penttila A (1975). Effects of fasting and feeding and pilocarpine on paneth cells of the mouse. *Scand J Gastroenterol* **10**, 347–352.

Au A, Gupta A, Schembri P & Cheeseman CI (2002). Rapid insertion of GLUT2 into the rat jejunal brush-border membrane promoted by glucagon-like peptide 2. *Biochem J* **367**, 247–254.

Baba R, Yamami M, Sakuma Y, Fujita M & Fujimoto S (2005). Relationship between glucose transporter and changes in the absorptive system in small intestinal absorptive cells during the weaning process. *Med Mol Morphol* **38**, 47–53.

Banno Y, Asano T & Nozawa Y (1994). Proteolytic modification of membrane-associated phospholipase C-β by μ-calpain enhances its activation by G-protein β γ subunits in human platelets. *FEBS Lett* **340**, 185–188.

Bezencon C, le Coutre J & Damak S (2007). Taste-signaling proteins are coexpressed in solitary intestinal epithelial cells. *Chem Senses* **32**, 41–49.

Caccia S, Casartelli M, Grimaldi A, Losa E, de Eguileor M, Pennacchio F & Giordana B (2007). The unexpected similarity of intestinal sugar absorption by SGLT1 and apical GLUT2 in an insect (Aphidius ervi, Hymenoptera) and mammals. *Am J Physiol Regul Integr Comp Physiol* epub ahead of print.

Caccia S, Leonardi MG, Casartelli M, Grimaldi A, de Eguileor M, Pennacchio F & Giordana B (2005). Nutrient absorption by *Aphidius ervi* larvae. *J Insect Physiol* **51**, 1183–1192.

Chen MC, Wu SV, Reeve JR Jr & Rozengurt E (2006). Bitter stimuli induce Ca^{2+} signaling and CCK release in enteroendocrine STC-1 cells: role of L-type voltage-sensitive Ca_{2+} channels. *Am J Physiol Cell Physiol* **291**, C726–C739.

Conigrave AD & Brown EM (2006). Taste receptors in the gastrointestinal tract. II. L-amino acid sensing by calcium-sensing receptors: implications for GI physiology. *Am J Physiol Gastrointest Liver Physiol* **291**, G753–G761.

Corpe CP, Basaleh MM, Affleck J, Gould G, Jess TJ & Kellett GL (1996). The regulation of GLUT5 and GLUT2 activity in the adaptation of intestinal brush-border fructose transport in diabetes. *Pflugers Arch* **432**, 192–201.

Delay ER, Hernandez NP, Bromley K & Margolskee RF (2006). Sucrose and monosodium glutamate taste thresholds and discrimination ability of T1R3 knockout mice. *Chem Senses* **31**, 351–357.

Dockray GJ (2003). Luminal sensing in the gut: an overview. *J Physiol Pharmacol* **54** (Suppl. 4), 9–17.

Dyer J, Salmon KS, Zibrik L & Shirazi-Beechey SP (2005). Expression of sweet taste receptors of the T1R family in the intestinal tract and enteroendocrine cells. *Biochem Soc Trans* **33**, 302–305.

Dyer J, Vayro S, King TP & Shirazi-Beechey SP (2003). Glucose sensing in the intestinal epithelium. *Eur J Biochem* **270**, 3377–3388.

Ferraris RP (2001). Dietary and developmental regulation of intestinal sugar transport. *Biochem J* **360**, 265–276.

Ferraris RP, Yasharpour S, Lloyd KC, Mirzayan R & Diamond JM (1990). Luminal glucose concentrations in the gut under normal conditions. *Am J Physiol Gastrointest Liver Physiol* **259**, G822–G837.

Gouyon F, Caillaud L, Carriere V, Klein C, Dalet V, Citadelle D, Kellett GL, Thorens B, Leturque A & Brot-Laroche E (2003). Simple-sugar meals target GLUT2 at enterocyte apical membranes to improve sugar absorption: a study in GLUT2-null mice. *J Physiol* **552**, 823–832.

Habold C, Foltzer-Jourdainne C, Le Maho Y, Lignot JH & Oudart H (2005). Intestinal gluconeogenesis and glucose transport according to body fuel availability in rats. *J Physiol* **566**, 575–586.

Helliwell PA & Kellett GL (2002). The active and passive components of glucose absorption in rat jejunum under low and high perfusion stress. *J Physiol* **544**, 579–589.

Helliwell PA, Richardson M, Affleck J & Kellett GL (2000*a*). Stimulation of fructose transport across the intestinal brush-border membrane by PMA is mediated by GLUT2 and dynamically regulated by protein kinase C. *Biochem J* **350**, 149–154.

Helliwell PA, Richardson M, Affleck J & Kellett GL (2000*b*). Regulation of GLUT5, GLUT2 and intestinal brush-border fructose absorption by the extracellular signal-regulated kinase, p38 mitogen-activated kinase and phosphatidylinositol 3-kinase intracellular signalling pathways: implications for adaptation to diabetes. *Biochem J* **350**, 163–169.

Helliwell PA, Rumsby MG & Kellett GL (2003). Intestinal sugar absorption is regulated by phosphorylation and turnover of protein kinase C βII mediated by phosphatidylinositol 3-kinase- and mammalian target of rapamycin-dependent pathways. *J Biol Chem* **278**, 28644–28650.

Hirsh AJ & Cheeseman CI (1998). Cholecystokinin decreases intestinal hexose absorption by a parallel reduction in SGLT1 abundance in the brush-border membrane. *J Biol Chem* **273**, 14545–14549.

Hofer D, Asan E & Drenckhahn D (1999). Chemosensory perception in the gut. *News Physiol Sci* **14**, 18–23.

Hofer D, Puschel B & Drenckhahn D (1996). Taste receptor-like cells in the rat gut identified by expression of α-gustducin. *Proc Natl Acad Sci U S A* **93**, 6631–6634.

Itoh Y, Kawamata Y, Harada M, Kobayashi M, Fujii R, Fukusumi S *et al.* (2003). Free fatty acids regulate insulin secretion from pancreatic β cells through GPR40. *Nature* **422**, 173–176.

Kellett GL (2001). The facilitated component of intestinal glucose absorption. *J Physiol* **531**, 585–595.

Kellett GL & Brot-Laroche E (2005). Apical GLUT2: a major pathway of intestinal sugar absorption. *Diabetes* **54**, 3056–3062.

Kellett GL & Helliwell PA (2000). The diffusive component of intestinal glucose absorption is mediated by the glucose-induced recruitment of GLUT2 to the brush-border membrane. *Biochem J* **350**, 155–162.

Khoursandi S, Scharlau D, Herter P, Kuhnen C, Martin D, Kinne RK & Kipp H (2004). Different modes of sodium-D-glucose cotransporter-mediated D-glucose uptake regulation in Caco-2 cells. *Am J Physiol Cell Physiol* **287**, C1041–C1047.

Kwon O, Eck P, Chen S, Corpe CP, Lee JH, Kruhlak M & Levine M (2006). Inhibition of the intestinal glucose transporter GLUT2 by flavonoids. *FASEB J* **21**, 366–377.

Li X, Staszewski L, Xu H, Durick K, Zoller M & Adler E (2002). Human receptors for sweet and umami taste. *Proc Natl Acad Sci U S A* **99**, 4692–4696.

Mace OJ, Morgan EL, Affleck JA, Lister N & Kellett GL (2007). Calcium absorption by Cav1.3 induces terminal web myosin II phosphorylation and apical GLUT2 insertion in rat intestine. *J Physiol* **580**, 605–616.

Margolskee RF (2002). Molecular mechanisms of bitter and sweet taste transduction. *J Biol Chem* **277**, 1–4.

Montmayeur JP, Liberles SD, Matsunami H & Buck LB (2001). A candidate taste receptor gene near a sweet taste locus. *Nat Neurosci* **4**, 492–498.

Morgan EL, Mace OJ, Affleck JA & Kellett GL (2007). Apical GLUT2 and Cav1.3: regulation of rat intestinal glucose and calcium absorption. *J Physiol* **580**, 593–604.

Morgan EL, Mace OJ, Helliwell PA, Affleck J & Kellett GL (2003). A role for $Ca_V1.3$ in rat intestinal calcium absorption. *Biochem Biophys Res Commun* **312**, 487–493.

Nelson G, Hoon MA, Chandrashekar J, Zhang Y, Ryba NJ & Zuker CS (2001). Mammalian sweet taste receptors. *Cell* **106**, 381–390.

Obin MS, Jahngen-Hodge J, Nowell T & Taylor A (1996). Ubiquitinylation and ubiquitin-dependent proteolysis in vertebrate photoreceptors (rod outer segments). Evidence for ubiquitinylation of Gt and rhodopsin. *J Biol Chem* **271**, 14473–14484.

Pappenheimer JR (1993). On the coupling of membrane digestion with intestinal absorption of sugars and amino acids. *Am J Physiol Gastrointest Liver Physiol* **265**, G409–G417.

Porter EM, Bevins CL, Ghosh D & Ganz T (2002). The multifaceted Paneth cell. *Cell Mol Life Sci* **59**, 156–170.

Raybould HE (1998). Does your gut taste? Sensory transduction in the gastrointestinal tract. *News Physiol Sci* **13**, 275–280.

Sbarbati A & Osculati F (2005). The taste cell-related diffuse chemosensory system. *Prog Neurobiol* **75**, 295–307.

Sharp PA, Debnam ES & Srai SK (1996). Rapid enhancement of brush border glucose uptake after exposure of rat jejunal mucosa to glucose. *Gut* **39**, 545–550.

Walker J, Jijon HB, Diaz H, Salehi P, Churchill T & Madsen K (2004). 5-Aminoimidazole-4-carboxamide riboside (AICAR) enhances GLUT2-dependent jejunal glucose transport: a possible role for AMPK. *Biochem J* **385**, 485–491.

Wu SV, Rozengurt N, Yang M, Young SH, Sinnett-Smith J & Rozengurt E (2002). Expression of bitter taste receptors of the T2R family in the gastrointestinal tract and enteroendocrine STC-1 cells. *Proc Natl Acad Sci U S A* **99**, 2392–2397.

Acknowledgements

This work was supported by The Wellcome Trust. O.J.M. was the recipient of a BBSRC studentship. We thank Dr Peter O'Toole (Director) and Dr Karen Chance of our department's Imaging and Cytometry Unit for invaluable assistance with the colocalization studies. We are grateful to Dr Emma Morgan for helpful comments during the course of this work.